

Shocklets and Short Large Amplitude Magnetic Structures (SLAMS) in the high Mach foreshock of Venus

Glyn A. Collinson^{1,2}, Heli Hietala³, Ferdinand Plaschke⁴, Tomas Karlsson⁵,
Lynn B. Wilson III¹, Martin Archer⁶, Markus Battarbee⁷, Xochitl
Blanco-Cano⁸, Cesar Bertucci⁹, David Long¹⁰, Merav Opher¹¹, Nick Sergis¹²,
Claire Gasque¹³, Terry Liu¹⁴, Savvas Raptis^{5,15}, Sofia Burne⁹, Rudy Frahm¹⁶,
Tielong Zhang¹⁷, Yoshifumi Futaana¹⁸

¹NASA Goddard Space Flight Center, Greenbelt, Maryland, USA

²The Catholic University of America, Washington, District of Columbia, USA

³School of Physical and Chemical Sciences, Queen Mary, University of London, London, UK

⁴Technische Universität Braunschweig, Braunschweig, Germany

⁵Division of Space and Plasma Physics, KTH Royal Institute of Technology, Stockholm, Sweden

⁶Faculty of Natural Sciences, Department of Physics, Imperial College London, London, UK

⁷Space Physics Research Group, University of Helsinki, Helsinki, Finland

⁸Instituto de Geofísica, Universidad Nacional Autónoma de México, Mexico City, Mexico

⁹Institute for Astronomy and Space Physics (IAFE), UBA CONICET Buenos Aires, Argentina

¹⁰Astrophysics Research Centre, Queen's University Belfast, Belfast, United Kingdom

¹¹Department of Astronomy, Boston University, Boston, Massachusetts, USA

¹²Hellenic Space Center, Chalandri, Greece

¹³Space Sciences Laboratory, University of California, Berkeley, California, USA

¹⁴Department of Earth Planetary and Space Sciences, University of California, Los Angeles, USA

¹⁵Applied Physics Laboratory, Johns Hopkins University, Laurel, Maryland, USA

¹⁶Southwest Research Institute, San Antonio, Texas, USA

¹⁷Space Research Institute, Austrian Academy of Sciences, Graz, Austria

¹⁸Institutet för Rymdfysik, Kiruna, Sweden

Key Points:

- Shocklets and SLAMS can form in the steady-state foreshock of Venus despite the magnetosphere being $1/10^{th}$ the size of Earths.
- The Venusian Shocklets and SLAMS had comparable magnetic signatures to those reported near Earth, but may be rarer.
- Analysis of the solar wind at 0.72AU suggests Shocklets and SLAMS occur during high Alfvén mach-numbers with a lower limit on occurrence rate of $\gtrsim 14\%$.

Corresponding author: Glyn Collinson, glyn.a.collinson@nasa.gov

Abstract

Shocklets and Short Large-Amplitude Magnetic Structures (SLAMS) are steepened magnetic fluctuations commonly found in Earth’s upstream foreshock. Here we present *Venus Express* observations from the 26th of February 2009 establishing their existence in the steady-state foreshock of Venus, building on a past study which found SLAMS during a substantial disturbance of the induced magnetosphere. The Venusian structures were comparable to those reported near Earth. The 2 Shocklets had magnetic compression ratios of 1.23 and 1.34 with linear polarization in the spacecraft frame. The 3 SLAMS had ratios between 3.22 and 4.03, two of which with elliptical polarization in the spacecraft frame. Statistical analysis suggests SLAMS coincide with unusually high solar wind Alfvén mach-number at Venus (12.5, this event). Thus, while we establish Shocklets and SLAMS can form in the stable Venusian foreshock, they may be rarer than at Earth. We estimate a lower limit of their occurrence rate of $\gtrsim 14\%$.

Plain Language Summary

We discover that Venus, like Earth, also has magnetic structures called Shocklets and SLAMS in its foreshock region, which is the area upstream of the planet where the interplanetary magnetic field is connected to its bow shock. Shocklets and SLAMS are common in the foreshock of Earth. However, Shocklets have not been observed at Venus before, and SLAMS have only been seen once, and then only during a large disturbance of the space near Venus. Thus it is unknown if SLAMS and Shocklets can form in the foreshock of a planet as close to its star as Venus. We used observations from the European Space Agency’s *Venus Express* orbiter (2006-2014) to identify these structures in the Venusian foreshock. The structures were found to be present during periods of high solar wind activity, and a lower limit on how often they occur is at least 14% of the time. These findings provide new insights into the space environment around Venus and may help us understand the differences in the space environments of different planets.

1 Introduction**1.1 The field of ultra-low-frequency (ULF) waves upstream of Venus**

A foreshock is the region that forms upstream of any planetary supersonic bow shock where the interplanetary magnetic field (IMF) is magnetically connected to the bow shock, i.e. parallel to the shock normal ($\theta_{B,\hat{n}} < 45^\circ$) (Eastwood, Lucek, et al., 2005). Under these conditions, and as long as the Alfvén Mach number exceeds ≈ 4 (Thomsen et al., 1993), ions reflected at the bow shock can escape back upstream. The resulting ion beam instabilities generate a field of ultra-low-frequency (ULF) waves which pervade the foreshock region (Fairfield, 1969; Scarf et al., 1970). They are often referred to as “30s waves” (Eastwood, Balogh, et al., 2005) due to their typical period at Earth (in the spacecraft frame), which comes from the strength and cone angle of the interplanetary magnetic field (Takahashi et al., 1984). A similar field of 30s ULF waves was discovered upstream of Venus by Greenstadt et al. (1987). They found the general morphology of the Venusian foreshock ULF wave field is similar to that at Earth despite the vastly different scale sizes of the planetary bow shocks. Statistical analysis by Shan et al. (2018) revealed their mean frequency to be 20 to 30s in the spacecraft frame (similar to Earth), 2 to 3 times the local proton cyclotron period. As at Earth, foreshock ULF waves originate in the quasi-parallel region of the Venusian foreshock (Omidi et al., 2017).

ULF waves attempt to propagate upstream from the planet they are generated near but are blown back towards the bow shock by the solar wind. As they move deeper into the foreshock, they encounter higher levels of superthermal ion density. These ions modify the refractive index of the medium, causing the transverse modes to become compressive, leading to the waves steepening (L. B. Wilson III et al., 2009; Tsubouchi & Lembège,

2004; Tsurutani et al., 1987). The waves become more oblique and compressive as they penetrate deeper into the foreshock. Two foreshock phenomena which can result from this steepening of ULF waves are (1) Shocklets (Hoppe & Russell, 1981) and (2) Short large-amplitude magnetic structures (SLAMS) (Schwartz, 1991; Chen et al., 2021).

1.2 Shocklets

1.2.1 Characteristics of Shocklets

As ULF waves are advected towards the bow shock, they can quickly grow to nonlinear amplitudes (Dorfman et al., 2017), undergoing steepening into “Shocklets”. Shocklets are magnetosonic magnetic structures with the following characteristics; (1) Magnetic compression ratio (dB/B_0) between 1 and 2 (L. B. Wilson et al., 2013); (2) Have a steepened upstream edge giving a “saw tooth” profile (Bertucci et al., 2007); (3) typically display linear polarization (Hoppe & Russell, 1981); and (4) dispersively radiate higher frequency electromagnetic whistler precursor waves as they steepen (L. B. Wilson et al., 2013).

1.2.2 Where have Shocklets been observed previously?

Shocklets were first reported at Earth by Hoppe and Russell (1981) and have since been observed at other magnetospheres including upstream of Jupiter (Tsurutani et al., 1993) and Saturn (Bertucci et al., 2007; Andrés et al., 2013). However, no Shocklets have been previously reported at Venus despite extensive exploration of the Venusian ULF wave field by NASA’s *Pioneer Venus Orbiter* (1978-1992) and ESA’s *Venus Express* orbiter (2006-2014).

1.3 Short Large-Amplitude Magnetic Structures (SLAMS)

1.3.1 Characteristics of SLAMS

Another non-linear magnetosonic structure that can evolve from the ULF wave field are Short Large-Amplitude Magnetic Structures (SLAMS) (Schwartz, 1991). SLAMS are characterized at Earth by (1) Magnetic compression ratio (dB/B_0) of at least twice the background field (and sometimes being as high as $dB/B_0 = 5$) (Schwartz, 1991; Schwartz et al., 1992; L. B. Wilson et al., 2013); (2) Brief (5–20s) monolithic spikes in magnetic field magnitude ($|B|$); (3) Elliptical polarization in the plasma frame (but can be observed as linear polarized in the spacecraft frame) (Schwartz, 1991; Tsurutani et al., 1993; Schwartz et al., 1992; Dubouloz & Scholer, 1993).

1.3.2 Where have SLAMS been observed previously?

The first extraterrestrial report of “steepened magnetosonic waves” consistent with SLAMS was made by Tsurutani et al. (1987), who used data from the *International Comet Explorer* spacecraft during its intercept with Comet Giacobini-Zinner at a distance from the Sun of 1.72AU. SLAMS-like structures have subsequently been reported at, Mars (Halekas et al., 2017; Fowler et al., 2018; Collinson et al., 2018; Shuvalov & Grigorenko, 2023) (~ 1.52 AU), Jupiter (Tsurutani et al., 1993) (~ 5.2 AU), and Saturn (Bebesi et al., 2019) (~ 9.54 AU).

To date, the only report of SLAMS forming sunward of Earth is by Collinson, Wilson, et al. (2012), who presented a case study of 3 SLAMS upstream of the bow shock of Venus (0.72 AU). However, these were associated with a transient event in the foreshock driven by a discontinuity in the interplanetary magnetic field (possibly a Hot Flow Anomaly (Collinson, Sibeck, et al., 2014) or similar). This foreshock transient substantially perturbed the Venusian induced magnetosphere, driving the bow shock outwards from its

128 typical location by $\approx 3000km$. Thus, SLAMS have only been reported at Venus dur-
 129 ing a substantial disturbance of the foreshock and induced magnetosphere. It is unclear
 130 if they can exist in the steady-state foreshock of Venus, e.g. when the solar wind, inter-
 131 planetary magnetic field, and magnetosphere are quiescent.

132 1.4 Objectives and overview of this paper

133 The dearth of observations of Shocklets and SLAMS in the steady-state foreshock of Venus
 134 calls into question whether they can form at such small magnetospheres under quiescent
 135 upstream conditions. Given that at Venus the bow shock is an order of magnitude smaller
 136 than at Earth it is not obvious whether ULF waves will have sufficient time and space
 137 to grow nonlinear and steepen into Shocklets and SLAMS. Thus, understanding under
 138 what conditions the Venusian foreshock can intrinsically generate such structures would
 139 be important for our understanding how stellar winds interact with small bow shocks,
 140 such as those found at planets and moons with induced magnetospheres (e.g. Venus, Mars,
 141 Titan), Comets, and worlds with weak magnetic dipoles (e.g. Mercury).

142 Here we present a case study of *in-situ* observations by ESA’s *Venus Express* orbiter from
 143 the 26th of February 2009, demonstrating the existence of both Shocklets and SLAMS
 144 in the steady-state foreshock and ULF wave field of Venus. We use data from the *Venus*
 145 *Express* Magnetometer (Zhang et al., 2006) and Analyzer for Space Plasmas and Ener-
 146 getic Atoms (ASPERA-4) Ion Mass Analyzer (IMA) (Barabash et al., 2007) and Elec-
 147 tron Spectrometer (ELS) (Collinson et al., 2009).

148 Our paper is outlined as follows. In Section 2 we give a brief review of the induced mag-
 149 netosphere and foreshock of Venus. In Section 3 we describe the *Venus Express* instru-
 150 ments used in this study. In Section 4 we describe orbit №1043 and give an overview of
 151 what conditions were like in the quasi-parallel magnetosheath and foreshock. In Section
 152 5 we describe our analysis of the 5 events (3 SLAMS and 2 Shocklet candidates). In sec-
 153 tion 6 we describe statistical analysis of solar wind measurements by *Venus Express*, find-
 154 ing that SLAMS and Shocklets may not be common at Venus. Finally in Section 7 we
 155 summarize our findings and conclusions.

156 2 The Venusian induced magnetosphere and foreshock

157 Without an intrinsic magnetic dipole (Smith et al., 1965a) the obstacle to the solar wind
 158 at Venus is its dense and conductive ionosphere. The advection of the interplanetary mag-
 159 netic field induces electrical currents within the ionosphere. These currents generate a
 160 global system of weak and overlapping induced magnetic fields (Dubinin et al., 2013).
 161 The resulting induced magnetosphere is far weaker than at Earth and roughly an order
 162 of magnitude smaller (Luhmann, 1990; Bertucci et al., 2011; Futaana et al., 2017). The
 163 Venusian bow shock stands off only ≈ 1.4 Venus Radii (R_V) upstream from the center
 164 of the planet (Slavin et al., 1980) (Figure 1G), as compared to $\approx 15R_E$ at Earth (Fairfield,
 165 1971). Behind the Venusian bow shock is the Magnetosheath (sometimes called the Ionosheath),
 166 a region of shock-heated solar wind. For more information on the structure of the Venu-
 167 sian magnetosphere (which has been recently revised in light of new data from *Parker*
 168 *Solar Probe*), see Collinson, Ramstad, et al. (2022).

169 The Venusian foreshock can extend for several R_V upstream of the planet, especially when
 170 the interplanetary magnetic field is aligned with the Venus-Sun axis (Luhmann et al.,
 171 1986; Omididi et al., 2017; Collinson et al., 2020). Our current understanding is that the
 172 Venusian foreshock is similar to Earth’s, albeit in miniature, containing the same tran-
 173 sient phenomena, including ULF Waves (Greenstadt et al., 1987; Dubinin & Fraenz, 2016;
 174 Fränz et al., 2017), Foreshock Whistler “1 Hz” waves (Orlowski et al., 1990; Collinson
 175 et al., 2015), Hot Flow Anomalies (Collinson, Sibeck, et al., 2012, 2014), Spontaneous
 176 Hot Flow Anomalies (Collinson et al., 2017), Foreshock Bubbles (Omididi et al., 2020), Fore-

177 shock Cavities (Collinson et al., 2020), and now SLAMS and Shocklets (This Study). Venus
 178 has an additional source of upstream waves, which can arise from the pickup of ions from
 179 the exosphere which at Venus extends into the solar wind (Delva et al., 2015).

180 **3 *Venus Express* Instrumentation**

181 The primary instrument used in this study is the *Venus Express* magnetometer (MAG)
 182 (Zhang et al., 2006), which measured 3D ambient magnetic fields at cadences of up to
 183 128Hz. In this study, standard survey data (4s) as well as high-resolution (32 Hz) data
 184 is used. This study is supported by measurements of electrons and ions by the Analyzer
 185 for Space Plasmas and Energetic Atoms (ASPERA-4) (Barabash et al., 2007; Collinson
 186 et al., 2009). ASPERA-ELS measured the energy spectra of electrons between 1eV and
 187 21keV at a cadence of either 1s or 4s. This study also uses solar wind measurements by
 188 the ASPERA-4 Ion Mass Analyzer (IMA) instrument, which measured the velocity distri-
 189 butions of ions between 12eV and 30keV. ASPERA-IMA had a broad 3D field of view
 190 ($90^\circ \times 360^\circ$), and the ability to separate ions by mass group (H^+ , He^+ , “Heavy ions”).
 191 However, ASPERA-IMA had a very slow (192 s) measurement cadence, and as will be
 192 shown in Section 6, tended to under-estimate solar-wind densities due to its $7\% \Delta E/E$
 193 energy bandpass.

194 **4 *Venus Express* explores the Venusian Foreshock on 26 February 2009**

195 Figure 1G shows a map of *Venus Express* orbit №1043, occurring on the 26th of Febru-
 196 ary 2009. Figures 1A-F show *in-situ* measurements from this orbit. Two time periods
 197 are shown. Figures 1A-C shows an overview of the entire encounter with the foreshock
 198 so that the events described in this paper can be put into context. Figures 1D-F shows
 199 a close up of 2 min 30 s of data containing Shocklets and SLAMS where we shall focus
 200 our analysis. Figures 1A,D show color coded timelines of each of these two periods. Mag-
 201 netometer (Mag) data (Fig. 1B,E) are presented in the Venus Solar Orbital (VSO) co-
 202 ordinate system, where x points towards the sun, y points back along the orbital path
 203 of the planet perpendicular to the Venus-Sun line opposite to the planet’s velocity vec-
 204 tor, and z points out of the plane of the ecliptic completing the right-hand set. The an-
 205 gles between the magnetic field and bow-shock normal ($\theta_{B,\hat{n}}$, Figure 1B,E) was calculated
 206 by propagating the IMF field line direction at the location of *Venus Express* until it in-
 207 tersects the Slavin et al. (1980) bow shock model. The Magnetic compression ratio (dB/B_0)
 208 was calculated by subtracting the 32Hz data from the time-averaged 1/4Hz data (B_0).

209 Data from the foreshock encounter (Fig. 1A-C) reveal there was no clear boundary de-
 210 lineation between the magnetosheath (maroon) and foreshock (dark blue). Large am-
 211 plitude waves were observed throughout the period (Fig 1B). These waves were of ap-
 212 proximately the same amplitude (30-40 nT) until $\approx 06:41$, after which they generally tended
 213 to reduce in amplitude with increasing distance from the planet. We thus estimate 06:41
 214 GMT as an approximate transition between being more in the sheath to being more in
 215 the foreshock, based also on a change in energy spectra from ASPERA-4 ELS (Fig 1C).
 216 These data are very consistent with the complex field of steepened magnetosonic waves
 217 expected in the quasi-parallel sheath and foreshock (Luhmann et al., 1987; Shan et al.,
 218 2014; Collinson et al., 2020). Thus, we conclude *Venus Express* transitioned between quasi-
 219 parallel magnetosheath to foreshock sometime after 06:41 GMT on the 26 of February
 220 2009, and was thus in the right place to search for SLAMS and Shocklets.

221 **5 SLAMS and Shocklets at Venus**

222 For the remainder of this paper we shall focus on magnetic fluctuations observed between
 223 06:44:00 and 06:46:30 GMT (light blue on Fig 1A timeline); 3 SLAMS (orange stars, Event
 224 №1, №2, №3); 2 Shocklets (Gold Circle, Event №5, №6); and 2 non-steepened ULF waves

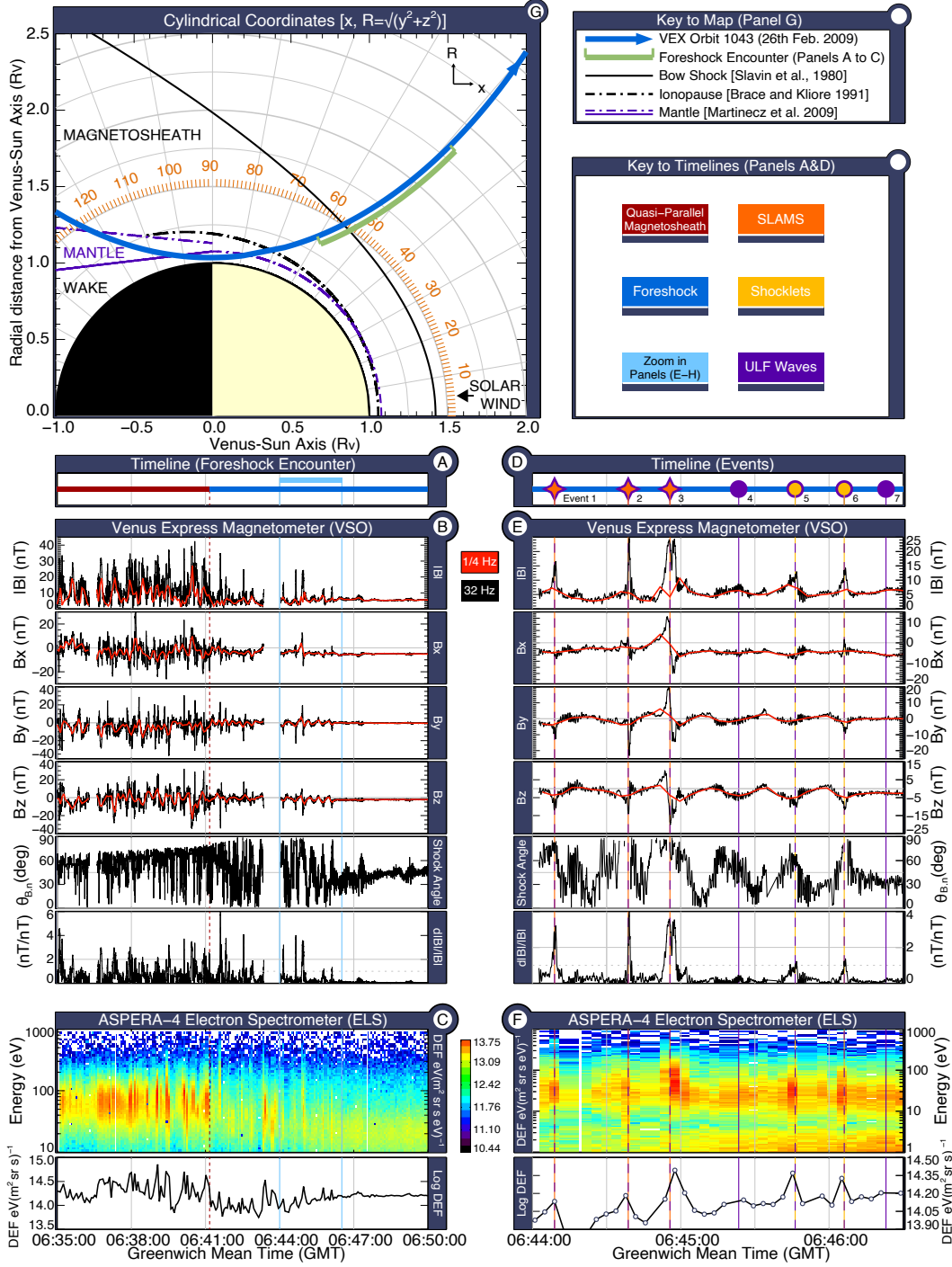


Figure 1. *Venus Express* field and particle observations from orbit №1043, 26th of February 2009. Panels A-C show data from the period 06:35 to 06:50, the time interval marked “Encounter” in Fig. 1G, covering the transition from magnetosheath to foreshock. Panels D-F show a zoom-in of the region of interest (06:44:00 to 06:46:30) where 3 SLAMS and 2 Shocklets candidates were encountered. Panels A&D show a color-coded timeline. Panels B&E show magnetometer (MAG) data at 32 Hz (black) and 1/4 Hz (red) cadence. From top to bottom; magnetic field magnitude ($|B|$) in nT; Vector (B_x , B_y , B_z , in VSO coordinates) in nT; the angle between the magnetic field and bow-shock normal ($\theta_{B,\hat{n}}$); and the compression ratio of the magnetic field (dB/B_0). Panels C&F show data from ASPERA-ELS, with time/energy spectrograms on top and the total measured superthermal Differential Energy Flux (DEF) below. Panel G shows a map of *Venus Express* orbit №1043 through the induced magnetosphere of Venus in units of Venus Radii ($R_V = 6051.8\text{km}$).

Event №	Classification	Start (GMT)	Duration (s)	dB/B_0	Polarization (S/C frame)	$\theta_{\hat{\mathbf{k}}\langle\hat{\mathbf{b}}\rangle}$	$\frac{\lambda_{mid}}{\lambda_{min}}$	$\frac{\lambda_{max}}{\lambda_{mid}}$
1	SLAMS	06:44:07	3.5 s	3.22	Linear	64.91°	3.82	13.21
2	SLAMS	06:44:38	2.0 s	4.03	Elliptical	89.27°	352.38	1.84
3	SLAMS	06:44:52	6.2 s	3.59	Elliptical	58.60°	95.23	3.17
5	Shocklet	06:45:40	8.4 s	1.23	Linear	78.71°	12.20	18.93
6	Shocklet	06:46:05	3.5 s	1.34	Linear	77.07°	9.14	7.88

Table 1. Table showing properties of the 5 steepened magnetosonic structures show in Fig. Duration was calculated by eye from the apparent start and stop time of the magnetic signature. Polarization was determined by eye from the hodogram in Fig. 2.

225 (Purple Circle, Event №4, №7) for comparison. These events were classified according
 226 to their compression ratios ($\delta B/B_0$).

227 5.1 Magnetometer

228 5.1.1 Overview of observations

229 A time-series of Magnetometer data are shown in Fig. 1B,E at two cadences; at 32 Hz
 230 (black) to better resolve the details of the magnetic perturbations; and at 1/4 Hz (bright
 231 red) to more clearly see the general trends in the background field. The first three events
 232 (№1, №2, №3) are highly compressive, all with $dB/B_0 > 3$, consistent with SLAMS.
 233 The compression ratio of event №2 was greater than the maximum factor of four for sim-
 234 ple compression (Gurnett & Bhattacharjee, 2005), also highly indicative of SLAMS (Schwartz
 235 et al., 1992).

236 The latter two events (№5 and №6) were less steep, with compression ratios between $1 <$
 237 $dB/B_0 \leq 2$, consistent with Shocklets. These two steepened waves were observed be-
 238 tween two ULF waves (№4, 7). Given all four were observed at a regular cadence of $20 \pm$
 239 $3s$ consistent with the period expected from the Venusian wave field (Shan et al., 2018),
 240 this suggests that the events №5 and №6 grew as a direct result of the steepening of “30
 241 s” ULF waves, as expected for Shocklets.

242 5.1.2 Minimum variance analysis of Venusian SLAMS and Shocklets

243 Following L. B. Wilson III et al. (2009) we performed minimum variance analysis (MVA)
 244 (Sönnnerup & Scheible, 1998) on each of the 3 SLAMS and 2 Shocklets using frequency
 245 filters to determine the characteristics of each magnetic structure. Figure 2 shows a close-
 246 up of magnetometer data from each of the events. The top panel shows calibrated mag-
 247 netometer data at 32 Hz in VSO coordinates (black, as per Fig. 1B&E). The bright red
 248 line shows these data with a $0.004 \rightarrow 0.5Hz$ filter applied. The lower panels of Fig. 2
 249 show hodograms of these filtered subintervals of data after MVA. Table 1 accompanies
 250 Fig. 2, showing the collected properties of each of the events, including the results of MVA
 251 analysis.

252 **SLAMS:** The top three panels (A,B,C) of Fig. 2 show close-ups of the three SLAMS
 253 candidates. The mean compression ratio of the SLAMS (dB/B_0) was 3.7 times the back-
 254 ground field, and they had periods between $\approx 2 \rightarrow 6$ s. The first SLAMS (Event №1)
 255 was linearly polarized in the spacecraft frame. The second and third SLAMS candidates
 256 (Event №2 and №3) were elliptically polarized in the spacecraft frame, consistent with
 257 previous observations of SLAMS (Dubouloz & Scholer, 1993; Mann et al., 1994). With
 258 only a single spacecraft we cannot determine the propagation direction. Of the three SLAMS

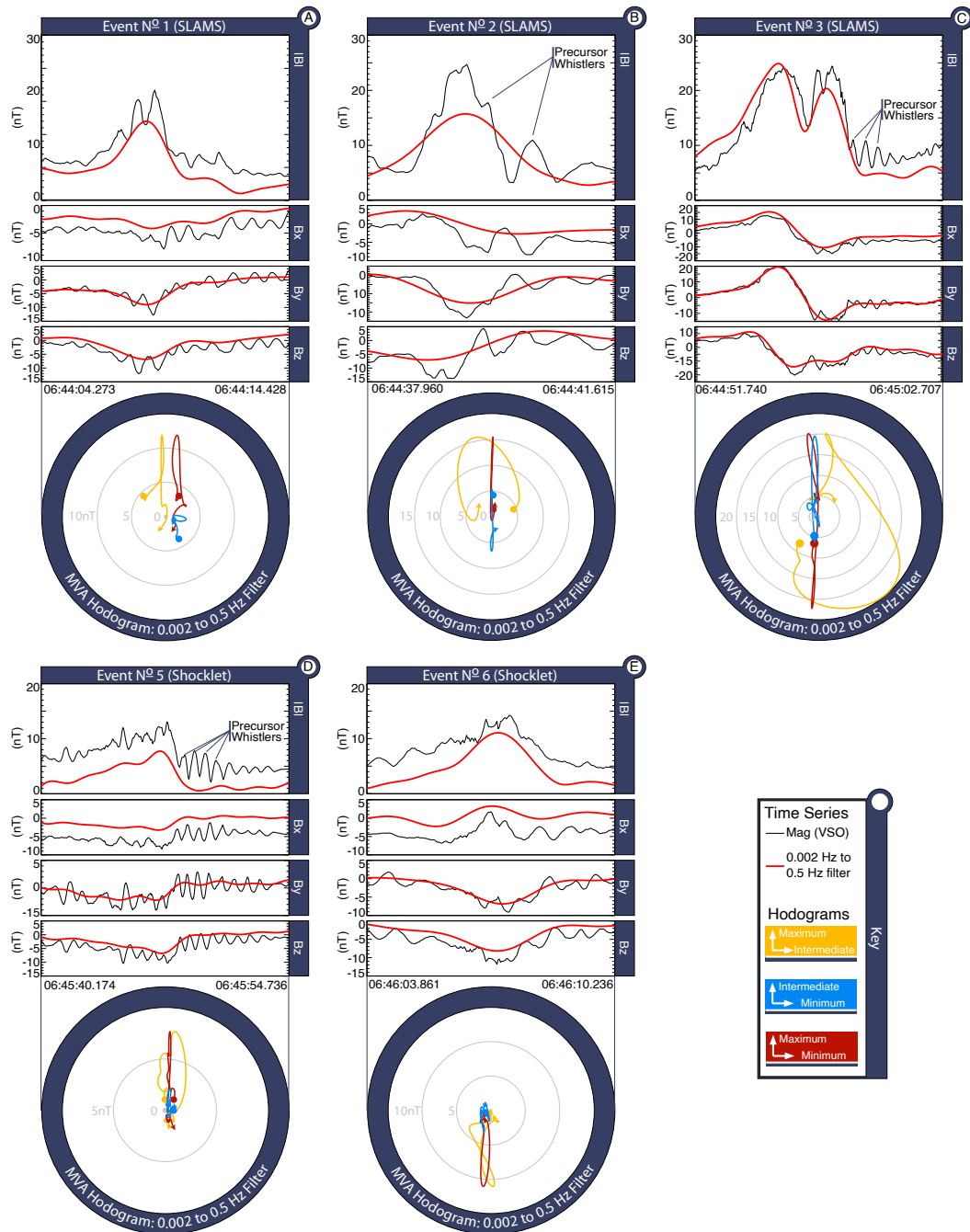


Figure 2. Close up view of the 3 SLAMS and 2 Shocklet candidates from Fig. 1E-H. Top Panels: time series showing original data and filtered between 0.002 Hz and 0.5 Hz. Bottom Panels: Hodogram of Minimum Variance Analysis of magnetometer data filtered between 0.002 Hz and 0.5 Hz.

259 candidates, event №2 exhibited the most circular polarization with MVA eigenvalues $\lambda_{mid}/\lambda_{min}$
 260 = 352 and $\lambda_{max}/\lambda_{mid} = 1.8$. Most of the five events are associated with a train of whistler
 261 waves, consistent with either SLAMS or Shocklets which act as a localized miniature bow
 262 shock. Of the SLAMS candidates, Event №3 shows the best example of a classical wave
 263 train of precursor whistlers on the upstream side, consistent with previous observations
 264 of SLAMS at Earth (L. B. Wilson et al., 2013) and Saturn (Bebesi et al., 2019). Our MVA
 265 analysis shows the three SLAMS candidates had an average angle between wave vector
 266 and the magnetic field of $\theta_{\hat{\mathbf{k}}\langle\hat{\mathbf{b}}\rangle} \approx 71^\circ$. These structures are thus compressive and obliquely
 267 propagating to the ambient magnetic field consistent with previous observations of SLAMS
 268 at Earth (Mann et al., 1994; Chen et al., 2021).

269 **Shocklets:** The bottom two panels (D,E) of Fig. 2 show close-ups of the two Shock-
 270 lets candidates. Both have the classical asymmetrical “saw-tooth” profile of a Shocklet,
 271 with a steeper edge on the upstream (trailing) side (Hoppe & Russell, 1981). The mean
 272 compression ratio was 1.29, and both were linearly polarized, also consistent with what
 273 is expected of Shocklets (L. B. Wilson et al., 2013). The two Shocklets had a similar $\theta_{\hat{\mathbf{k}}\langle\hat{\mathbf{b}}\rangle}$
 274 of $\approx 78^\circ$, which, again, is highly consistent with a fast magnetospheric mode structure
 275 such as a Shocklet.

276 5.2 Observations of associated plasma perturbations by the Electron Spec- 277 trometer (ASPERA-4 ELS)

278 A feature of compressive magnetosonic structures such as SLAMS and Shocklets is that
 279 they act like a local quasi perpendicular shock, locally perturbing the solar wind, and
 280 increasing both $|B|$ and plasma density (Dubouloz & Scholer, 1993; Mann et al., 1994;
 281 Behlke et al., 2003; Collinson et al., 2018). However, the previous study of SLAMS at
 282 Venus by Collinson, Wilson, et al. (2012) were unable to examine the the plasma per-
 283 turbations anticipated from SLAMS. Figures 1C&F show measurements of superther-
 284 mal electron flux from ASPERA-4 ELS, with a time/energy spectrogram on top and line-
 285 plot of total integrated superthermal electron flux at the bottom. Electron flux remained
 286 fairly constant during the two ULF waves (event №4 and №7). However electron flux was
 287 enhanced in phase with $|B|$ at all 3 SLAMS and both Shocklets, consistent with such
 288 steepened magnetosonic structures.

289 6 How common are SLAMS and Shocklets at Venus?

290 SLAMS have now been reported at Venus on two days: 11 April 2009 (Collinson, Wil-
 291 son, et al., 2012) and 26 February 2009 (this study). A thorough statistical determina-
 292 tion of the occurrence rate would require more than 2 events. However, following Collinson,
 293 Sibeck, et al. (2014) and Collinson, Fedorov, et al. (2014), we can put a lower limit on
 294 their occurrence rate through investigation of whether the conditions in the solar wind
 295 upstream of Venus were unusual on these two days. Specifically, we examine the solar
 296 wind Alfvén Mach number (M_A), which is thought to be a general requirement for SLAMS
 297 formation at Earth ($M_A \geq 4$) to reflect ions at the bow shock and set up the ion-ion
 298 beam instabilities that lead to ULF wave formation (Thomsen et al., 1993) from which
 299 SLAMS form.

300 Figure 3 shows histograms of the upstream conditions at Venus from the entire 2006-2014
 301 *Venus Express* mission (black). The data are further divided into two types: “slow” so-
 302 lar wind (with bulk velocities $< 500 \text{ km s}^{-1}$) and “fast” solar wind (with bulk veloc-
 303 ities $\geq 500 \text{ km s}^{-1}$) (Stakhiv et al., 2015; Collinson, Chen, et al., 2022). Using the strength
 304 of the interplanetary magnetic field ($|B|$), solar wind mass density (n_i , calculated using
 305 only proton solar wind data from IMA), and velocity ($|V|$), we can compute the Alfvén
 306 speed (V_A) and the Alfvén Mach Number (M_A) according to Equation 1.

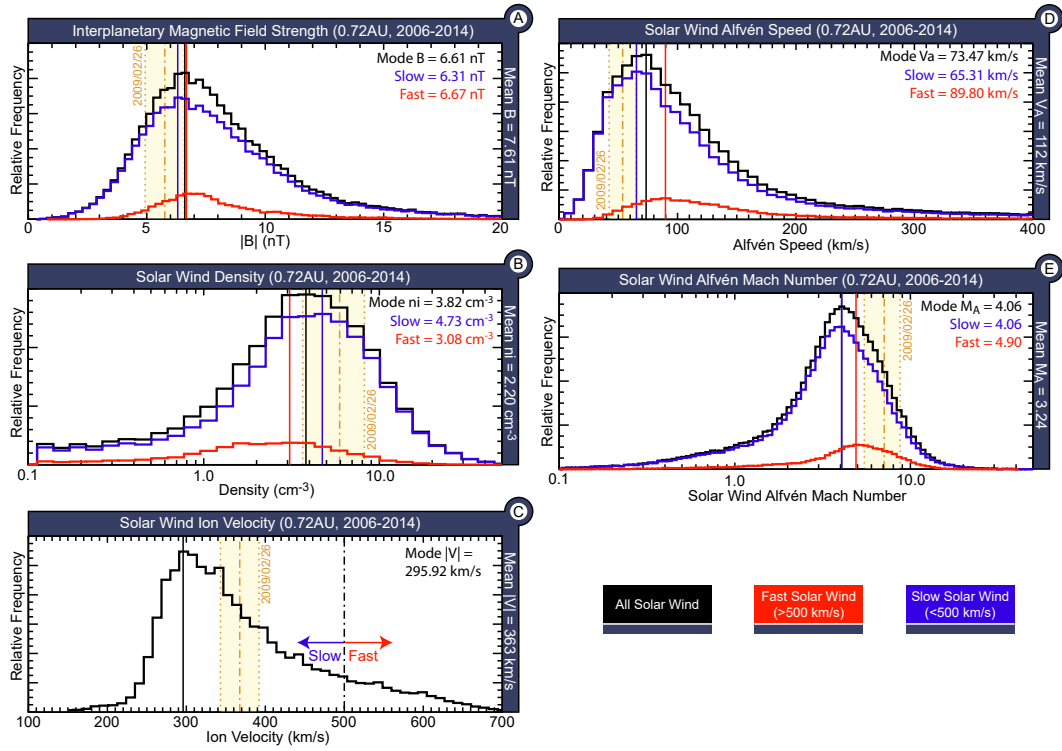


Figure 3. Histograms of properties of the interplanetary magnetic field and solar wind upstream of Venus as measured by *Venus Express* between 2006-2014. Panel A shows the strength of the IMF ($|B|$) from MAG. Panels B and C show solar wind proton density and velocity from ASPERA-4 IMA. Panels D and E show the Alfvén speed and Alfvén Mach Number (as measured, M_A) computed from these properties. Light yellow shading on each panel shows the conditions on 26 February 2009 (this study). Modal averages for each parameter are printed top right of each Panel, and the Mean value for each parameter is printed in the border.

$$M_A \equiv |V| \left(\frac{4\pi n_i}{|B|^2} \right)^{1/2} \quad (1)$$

307 Before we discuss M_A during SLAMS observation, we note that our analysis reveals that
 308 ASPERA-4 IMA substantially underestimated solar wind n_i . As shown in Figure 3B,
 309 the mean solar wind n_i reported by ASPERA-4 IMA at 0.72 AU was 2.2cm^{-3} , and the
 310 mode was 3.8cm^{-3} , much lower than the expected value of $\approx 12\text{cm}^{-3}$ (Köhnlein, 1996).
 311 We posit several potential contributing factors to this: (1) All “top hat” analyzers (such
 312 as ASPERA-4 IMA) can struggle to accurately measure the absolute densities of quasi-
 313 monoenergetic plasma beams such as the solar wind. (2) The field of view of ASPERA-
 314 4 IMA was frequently obscured by a thruster; (3) ASPERA-IMA was designed to mea-
 315 sure diffuse low energy oxygen ions escaping down the Martian and Venusian magneto-
 316 tails, and would thus sometimes saturate in the high-flux beam of the solar wind.

317 Assuming that the mean density was in reality closer to the expected value of $\approx 12\text{cm}^{-3}$
 318 and that this error is a linear systematic bias, then we can multiply the n_i measured by
 319 ASPERA-4 IMA by $\approx \times 3.1$ to make a rough estimate of the actual density (n_i^*). As
 320 per Equation 1, this suggests ASPERA-4 IMA also underestimated the Alfvén Mach num-
 321 ber by a factor of $\approx \times 1.77$. However, we caution that given the multiple possible con-
 322 tributing factors to the underestimation of solar wind density by ASPERA-IMA (par-
 323 ticularly detector saturation), the true bias is unlikely to be this linear and simple.

324 With this caveat, we find that M_A was unusually high on 26 February 2009, with a mean
 325 of 7.10 (measured), in the top 14% of the distribution of all measurements of M_A by *Venus*
 326 *Express* (Fig. 3E), and with an actual value possibly closer to $M_A^* \approx 12.5$. Likewise,
 327 when we computed M_A for 11 April 2009 (e.g. conditions during the Collinson, Wilson,
 328 et al. (2012) SLAMS case study) we find a similarly high mach number of 7.17, which
 329 is in the top 12% of the distribution of all measurements of M_A by *Venus Express* (Fig.
 330 3E), with an estimated actual value of $M_A^* \approx 12.7$.

331 To investigate whether this apparent dependence on SLAMS/Shocklet formation on high
 332 M_A is significant, we ran a one-way analysis of the variance (ANOVA) test on the fol-
 333 lowing two datasets: (1) Solar wind M_A on the two days where SLAMS have so far been
 334 identified; (2) M_A from the entire mission (Fig. 3E). The probability of measuring such
 335 high M_A on both days by random chance (The “P-value”) is 1.2×10^{-4} , i.e., very small.
 336 We thus show that M_A on these two days were statistical outliers at Venus.

337 This suggests that solar wind Alfvén mach number is likely important for SLAMS (and
 338 Shocklet) formation at Venus. This is generally in-line with what is expected from Earth
 339 where SLAMS and Shocklets tend to be associated with a higher M_A (Burgess & Scholer,
 340 2013). However, these observations may suggest that the M_A apparently required for their
 341 formation at Venus may be exceptionally high for 0.72AU (upper limit of $M_A^* \lesssim 12.5$),
 342 corresponding to a lower limit on occurrence rate of $\gtrsim 14\%$ of the time. This strongly
 343 motivates further statistical analysis to more thoroughly establish their occurrence rate
 344 at Venus, and their dependence on solar wind Alfvén mach number.

345 7 Summary and Discussion

346 In this paper we report the first observation of Shocklets at Venus, and demonstrate that
 347 SLAMS can form in the steady-state quasi-parallel Venusian foreshock, despite the mag-
 348 netosphere being $1/10^{\text{th}}$ smaller than at Earth. Thus we presume one would need to go
 349 to an even smaller system to determine the limit in scale-size below which such steep-
 350 ened foreshock structures do not have sufficient time to form.

- 351 1. Both SLAMS and Shocklet candidates were observed in the quasi-parallel fore-
 352 shock, the region where they are found at Earth.

- 353 2. MVA analysis revealed that all candidates propagated obliquely to the ambient
 354 field with $\theta_{\mathbf{k},\mathbf{b}}$ between 58.6° and 89.27° , consistent with SLAMS and Shocklets
 355 (Mann et al., 1994).
- 356 3. Two events exhibited the following characteristics consistent with Shocklets.
- 357 (a) They were of classic “sawtooth” appearance with a steeper upstream (trailing)
 358 edge (Hoppe & Russell, 1981).
- 359 (b) They were found in the field of 30s ULF waves, and appear to have replaced
 360 two wave crests, suggesting they have steepened directly out of 30s waves.
- 361 (c) Both candidates exhibited compression ratios (dB/B_0) of 1.3, consistent with
 362 Shocklets (higher than 1 but less than 2 (L. B. Wilson et al., 2013)).
- 363 (d) Both candidates were linearly polarized in the spacecraft frame
- 364 4. Three events exhibited the following characteristics consistent with SLAMS.
- 365 (a) Presented as large-amplitude monolithic spikes in $|B|$ that have compression
 366 ratios (dB/B_0) between $3.2 \Rightarrow 4.0$, with an average of 3.7, consistent with ter-
 367 restrial SLAMS which have $dB/B_0 \geq 2$ above the background field. (Schwartz
 368 et al., 1992; Mann et al., 1994).
- 369 (b) Two events were elliptically left-hand polarized in the spacecraft frame consis-
 370 tent with previous observations (Lucek et al., 2004, 2008).

371 We additionally demonstrated for the first time plasma perturbations associated with
 372 Venusian SLAMS and Shocklets. We expect such fast magnetosonic mode structures to
 373 be highly compressional, and increasing both $|B|$ and plasma density in phase with each
 374 other. We found electron flux to unambiguously increase with $|B|$, consistent with what
 375 is expected during both SLAMS and Shocklets.

376 Through statistical analysis of all solar wind measurements by *Venus Express* we found
 377 that solar wind Alfvén Mach number (M_A) was unusually high both for the SLAMS dis-
 378 covered in this study and those found by Collinson, Wilson, et al. (2012). Our results
 379 strongly suggest that high solar wind mach number is a driver of SLAMS formation at
 380 Venus. More than 2 events are required to establish a true occurrence rate. However, if
 381 we assume that the mach number for this event ($M_A^* = 12.5$) is the lower limit, this
 382 corresponds to a lower limit on the occurrence rate of $\gtrsim 14\%$ of the time. As solar wind
 383 mach number generally increases with distance from the sun, we posit this suggests that
 384 SLAMS may be more common at foreshocks at greater Heliospheric distances. Conversely,
 385 SLAMS and Shocklets may be less common the closer a planet orbits a star. However,
 386 we acknowledge there are significant uncertainties in these numerical estimations, and
 387 further analysis is needed to more thoroughly establish an occurrence rate.

388 Our analysis reveals ASPERA-4 IMA substantially underestimated ion density (n_i) in
 389 the solar wind by a factor of $\approx \times 3.1$, and thus future users of this dataset should be cau-
 390 tious when using the absolute densities it apparently measured, as these may be an un-
 391 derestimation.

392 Steepened foreshock wave structures (similar to SLAMS) have been shown to directly
 393 impact the upper ionosphere of Mars (Fowler et al., 2018; Collinson et al., 2018), and
 394 a similar process has been suggested at Venus (Collinson et al., 2020). Thus further ex-
 395 ploration of the Venusian foreshock is necessary to (1) understand the occurrence rate
 396 of SLAMS and Shocklets; (2) understand how they perturb space near Venus; and (3)
 397 how their impact on the ionopause affects the unshielded ionosphere below.

398 Acknowledgments

399 G.A.C. and R.F. were supported by a grant from the NASA ROSES Solar System Work-
 400 ings program (grant N^o80NSSC20K0317). H.H. is supported by the Royal Society Uni-
 401 versity Research Fellowship URF/R1/180671. M.A. was supported by UKRI (STFC /

402 EPSRC) Stephen Hawking Fellowship EP/T01735X/1. D.M.L. is grateful to the Science
 403 Technology and Facilities Council for the award of an Ernest Rutherford Fellowship (ST/R003246/1).
 404 This research was supported by the International Space Science Institute (ISSI) in Bern,
 405 through ISSI International Team project №465 “Foreshocks Across The Heliosphere: Sys-
 406 tem Specific Or Universal Physical Processes?”. We acknowledge and thank the front-
 407 line healthcare workers of our respective countries for their service during the COVID-
 408 19 pandemic, the beginning of which coincided with the initiation of this study.

409 Open Research

410 Venus Express Ephemeris data and calibrated ASPERA-ELS data can be found by typ-
 411 ing “Venus Express [mission]” into the search bar at the European Space Agency Plan-
 412 etary Science Archive (PSA) (<https://archives.esac.esa.int/psa>).

413 References

- 414 Andrés, N., Gómez, D. O., Bertucci, C., Mazelle, C., & Dougherty, M. K. (2013,
 415 May). Saturn’s ULF wave foreshock boundary: Cassini observations. *Planet.*
 416 *Space. Sci.*, *79*, 64-75. doi: 10.1016/j.pss.2013.01.014
- 417 Barabash, S., Sauvaud, J.-A., Gunell, H., Andersson, H., Grigoriev, A., Brinkfeldt,
 418 K., ... Bochsler, P. (2007, October). The Analyser of Space Plasmas and
 419 Energetic Atoms (ASPERA-4) for the Venus Express mission. *Planet. Space.*
 420 *Sci.*, *55*, 1772-1792.
- 421 Bebesi, Z., Erdos, G., & Szego, K. (2019, November). Observations of short large
 422 amplitude magnetic structures at the Kronian bow shock. *Icarus*, *333*, 306-
 423 317. doi: 10.1016/j.icarus.2019.06.023
- 424 Behlke, R., André, M., Buchert, S. C., Vaivads, A., Eriksson, A. I., Lucek, E. A., &
 425 Balogh, A. (2003, February). Multi-point electric field measurements of Short
 426 Large-Amplitude Magnetic Structures (SLAMS) at the Earth’s quasi-parallel
 427 bow shock. *Geophys. Res. Lett.*, *30*(4), 040000-1.
- 428 Bertucci, C., Achilleos, N., Mazelle, C., Hospodarsky, G. B., Thomsen, M.,
 429 Dougherty, M. K., & Kurth, W. (2007, September). Low-frequency waves
 430 in the foreshock of Saturn: First results from Cassini. *Journal of Geophysical*
 431 *Research (Space Physics)*, *112*(A9), A09219. doi: 10.1029/2006JA012098
- 432 Bertucci, C., Duru, F., Edberg, N., Fraenz, M., Martinecz, C., Szego, K., & Vais-
 433 berg, O. (2011, December). The Induced Magnetospheres of Mars, Venus, and
 434 Titan. *Space Sci. Rev.*, *162*(1-4), 113-171. doi: 10.1007/s11214-011-9845-1
- 435 Burgess, D., & Scholer, M. (2013, October). Microphysics of Quasi-parallel Shocks in
 436 Collisionless Plasmas. *Space Sci. Rev.*, *178*(2-4), 513-533. doi: 10.1007/s11214
 437 -013-9969-6
- 438 Chen, L.-J., Wang, S., Ng, J., Bessho, N., Tang, J.-M., Fung, S. F., ... Burch,
 439 J. (2021, January). Solitary Magnetic Structures at Quasi-Parallel Col-
 440 lisionless Shocks: Formation. *Geophys. Res. Lett.*, *48*(1), e90800. doi:
 441 10.1029/2020GL090800
- 442 Collinson, G. A., Chen, L.-J., Jian, L. K., & Dorelli, J. (2022, March). The Solar
 443 Wind at (16) Psyche: Predictions for a Metal World. *Astrophysical Journal*,
 444 *927*(2), 202. doi: 10.3847/1538-4357/ac51d7
- 445 Collinson, G. A., Fedorov, A., Futaana, Y., Masunaga, K., Hartle, R., Stenberg, G.,
 446 ... Zhang, T. L. (2014, August). The extension of ionospheric holes into the
 447 tail of Venus. *Journal of Geophysical Research (Space Physics)*, *119*, 6940-
 448 6953. doi: 10.1002/2014JA019851
- 449 Collinson, G. A., Grebowsky, J., Sibeck, D. G., Jian, L. K., Boardsen, S., Espley, J.,
 450 ... Kollmann, P. (2015, April). The impact of a slow Interplanetary Coro-
 451 nal Mass Ejection (ICME) on Venus. *Journal of Geophysical Research: Space*
 452 *Physics*. doi: 10.1002/2014JA020616
- 453 Collinson, G. A., Kataria, D. O., Coates, A. J., Tsang, S. M. E., Arridge, C. S.,

- 454 Lewis, G. R., ... Barabash, S. (2009, May). Electron optical study of the
 455 Venus Express ASPERA-4 Electron Spectrometer (ELS) top-hat electrostatic
 456 analyser. *Measurement Science and Technology*, *20*(5), 055204+.
- 457 Collinson, G. A., Ramstad, R., Frahm, R., Wilson, L., Xu, S., Whittlesey, P.,
 458 ... Ledvina, S. (2022, January). A Revised Understanding of the Structure
 459 of the Venusian Magnetotail From a High-Altitude Intercept With a
 460 Tail Ray by Parker Solar Probe. *Geophys. Res. Lett.*, *49*(1), e96485. doi:
 461 10.1029/2021GL096485
- 462 Collinson, G. A., Sibeck, D., Omid, N., Frahm, R., Zhang, T., Mitchell, D., ...
 463 Jakosky, B. (2020, August). Foreshock Cavities at Venus and Mars.
 464 *Journal of Geophysical Research (Space Physics)*, *125*(8), e28023. doi:
 465 10.1029/2020JA028023
- 466 Collinson, G. A., Sibeck, D., Omid, N., Grebowsky, J., Halekas, J., Mitchell, D., ...
 467 Jakosky, B. (2017, October). Spontaneous hot flow anomalies at Mars and
 468 Venus. *Journal of Geophysical Research (Space Physics)*, *122*, 9910-9923. doi:
 469 10.1002/2017JA024196
- 470 Collinson, G. A., Sibeck, D. G., Masters, A., Shane, N., Slavin, J. A., Coates, A. J.,
 471 ... Barabash, S. (2012, April). Hot Flow Anomalies at Venus. *Journal of*
 472 *Geophysical Research (Space Physics)*, *117*(A16), 4204.
- 473 Collinson, G. A., Sibeck, D. G., Masters, A., Shane, N., Zhang, T. L., Fedorov,
 474 A., ... Sarantos, M. (2014, February). A survey of hot flow anomalies at
 475 Venus. *Journal of Geophysical Research (Space Physics)*, *119*, 978-991. doi:
 476 10.1002/2013JA018863
- 477 Collinson, G. A., Wilson, L. B., Omid, N., Sibeck, D., Espley, J., Fowler, C. M., ...
 478 Jakosky, B. (2018, September). Solar Wind Induced Waves in the Skies of
 479 Mars: Ionospheric Compression, Energization, and Escape Resulting From the
 480 Impact of Ultralow Frequency Magnetosonic Waves Generated Upstream of the
 481 Martian Bow Shock. *Journal of Geophysical Research (Space Physics)*, *123*,
 482 7241-7256. doi: 10.1029/2018JA025414
- 483 Collinson, G. A., Wilson, L. B., III, Sibeck, D. G., Shane, N., Zhang, T. L., Moore,
 484 T. E., ... Barabash, S. (2012, October). Short large-amplitude magnetic struc-
 485 tures (SLAMS) at Venus. *Journal of Geophysical Research (Space Physics)*,
 486 *117*(A16), 10221.
- 487 Delva, M., Bertucci, C., Volwerk, M., Lundin, R., Mazelle, C., & Romanelli, N.
 488 (2015, January). Upstream proton cyclotron waves at Venus near solar max-
 489 imum. *Journal of Geophysical Research (Space Physics)*, *120*, 344-354. doi:
 490 10.1002/2014JA020318
- 491 Dorfman, S., Hietala, H., Astfalk, P., & Angelopoulos, V. (2017, March). Growth
 492 rate measurement of ULF waves in the ion foreshock. *Geophys. Res. Lett.*,
 493 *44*(5), 2120-2128. doi: 10.1002/2017GL072692
- 494 Dubinin, E., & Fraenz, M. (2016, February). Ultra-Low-Frequency Waves at Venus
 495 and Mars. *Washington DC American Geophysical Union Geophysical Mono-*
 496 *graph Series*, *216*, 343-364. doi: 10.1002/9781119055006.ch20
- 497 Dubinin, E., Fraenz, M., Woch, J., Zhang, T. L., Wei, Y., Fedorov, A., ...
 498 Lundin, R. (2013, October). Toroidal and poloidal magnetic fields at
 499 Venus. Venus Express observations. *Planet. Space. Sci.*, *87*, 19-29. doi:
 500 10.1016/j.pss.2012.12.003
- 501 Dubouloz, N., & Scholer, M. (1993, April). On the origin of short large-amplitude
 502 magnetic structures upstream of quasi-parallel collisionless shocks. *Geophys.*
 503 *Res. Lett.*, *20*, 547-550.
- 504 Eastwood, J. P., Balogh, A., Lucek, E. A., Mazelle, C., & Dandouras, I. (2005,
 505 November). Quasi-monochromatic ULF foreshock waves as observed by the
 506 four-spacecraft Cluster mission: 2. Oblique propagation. *J. Geophys. Res.*,
 507 *110*(A9), 11220.
- 508 Eastwood, J. P., Lucek, E. A., Mazelle, C., Meziane, K., Narita, Y., Pickett, J., &

- 509 Treumann, R. A. (2005, June). The Foreshock. *Space Sci. Rev.*, *118*, 41-94.
- 510 Fairfield, D. H. (1969). Bow shock associated waves observed in the far upstream in-
511 terplanetary medium. *J. Geophys. Res.*, *74*, 3541-3553.
- 512 Fairfield, D. H. (1971). Average and unusual locations for the earth's magnetopause
513 and bow shock. *J. Geophys. Res.*, *76*, 6700-6716.
- 514 Fowler, C. M., Andersson, L., Ergun, R. E., Harada, Y., Hara, T., Collinson, G.,
515 ... Jakosky, B. M. (2018, May). MAVEN Observations of Solar Wind-
516 Driven Magnetosonic Waves Heating the Martian Dayside Ionosphere.
517 *Journal of Geophysical Research (Space Physics)*, *123*, 4129-4149. doi:
518 10.1029/2018JA025208
- 519 Fränz, M., Echer, E., Marques de Souza, A., Dubinin, E., & Zhang, T. L. (2017,
520 October). Ultra low frequency waves at Venus: Observations by the
521 Venus Express spacecraft. *Planet. Space. Sci.*, *146*, 55-65. doi: 10.1016/
522 j.pss.2017.08.011
- 523 Futaana, Y., Stenberg Wieser, G., Barabash, S., & Luhmann, J. G. (2017, Novem-
524 ber). Solar Wind Interaction and Impact on the Venus Atmosphere. *Space Sci.*
525 *Rev.*, *212*(3-4), 1453-1509. doi: 10.1007/s11214-017-0362-8
- 526 Greenstadt, E. W., Baum, L. W., Jordan, K. F., & Russell, C. T. (1987, Apr).
527 The compressional ULF foreshock boundary of Venus: observations by
528 the PVO magnetometer. *J. Geophys. Res.*, *92*(A4), 3380-3384. doi:
529 10.1029/JA092iA04p03380
- 530 Gurnett, D. A., & Bhattacharjee, A. (2005). *Introduction to Plasma Physics*. Cam-
531 bridge University Press.
- 532 Halekas, J. S., Ruhunusiri, S., Harada, Y., Collinson, G., Mitchell, D. L., Mazelle,
533 C., ... Jakosky, B. M. (2017, January). Structure, dynamics, and seasonal
534 variability of the Mars-solar wind interaction: MAVEN Solar Wind Ion Ana-
535 lyzer in-flight performance and science results. *Journal of Geophysical Research*
536 *(Space Physics)*, *122*(1), 547-578. doi: 10.1002/2016JA023167
- 537 Hoppe, M., & Russell, C. (1981). On the nature of ULF waves upstream of plane-
538 tary bow shocks. *Advances in Space Research*, *1*(1), 327 - 332.
- 539 Köhnlein, W. (1996, November). Radial dependence of solar wind parameters in
540 the ecliptic (1.1 R \odot -61 AU). *Solar Physics*, *169*(1), 209-213. doi: 10.1007/
541 BF00153841
- 542 Lucek, E. A., Horbury, T. S., Balogh, A., Dandouras, I., & Rème, H. (2004, June).
543 Cluster observations of Hot Flow Anomalies. *Journal of Geophysical Research*
544 *(Space Physics)*, *109*(A18), A06207.
- 545 Lucek, E. A., Horbury, T. S., Dandouras, I., & Rème, H. (2008, June). Cluster ob-
546 servations of the Earth's quasi-parallel bow shock. *Journal of Geophysical Re-*
547 *search (Space Physics)*, *113*(A12), 7.
- 548 Luhmann, J. G. (1990, January). The solar wind interaction with unmagnetized
549 planets - A tutorial. *Geophysical Monograph Series*, *58*, 401-411. doi: 10.1029/
550 GM058p0401
- 551 Luhmann, J. G., Russell, C. T., & Elphic, R. (1986, February). Spatial Distributions
552 of Magnetic field fluctuations in the Dayside magnetosheath. *J. Geophys. Res.*,
553 *91*, 1711-1715.
- 554 Luhmann, J. G., Russell, C. T., Phillips, J. L., & Barnes, A. (1987, March). On the
555 role of the quasi-parallel bow shock in ion pickup - A lesson from Venus? *J.*
556 *Geophys. Res.*, *92*, 2544-2550.
- 557 Mann, G., Luehr, H., & Baumjohann, W. (1994, January). Statistical analysis of
558 short large-amplitude magnetic field structures in the vicinity of the quasi-
559 parallel bow shock. *J. Geophys. Res.*, *99*, 13315.
- 560 Omid, N., Collinson, G., & Sibeck, D. (2017). Structure and Properties of the
561 Foreshock at Venus. *Journal of Geophysical Research: Space Physics*, *122*(10),
562 10,275–10,286. doi: 10.1002/2017JA024180
- 563 Omid, N., Collinson, G., & Sibeck, D. (2020, February). Foreshock Bubbles at

- 564 Venus: Hybrid Simulations and VEX Observations. *Journal of Geophysical Re-*
565 *search (Space Physics)*, 125(2), e27056. doi: 10.1029/2019JA027056
- 566 Orłowski, D. S., Crawford, G. K., & Russell, C. T. (1990, December). Up-
567 stream waves at Mercury, Venus and earth - Comparison of the prop-
568 erties of one Hertz waves. *Geophys. Res. Lett.*, 17, 2293-2296. doi:
569 10.1029/GL017i013p02293
- 570 Scarf, F. L., Fredricks, R. W., Frank, L. A., Russell, C. T., Coleman, P. J., Jr., &
571 Neugebauer, M. (1970). Direct correlations of large-amplitude waves with
572 suprathermal protons in the upstream solar wind. *J. Geophys. Res.*, 75, 7316-
573 7322.
- 574 Schwartz, S. J. (1991). Magnetic field structures and related phenomena at quasi-
575 parallel shocks. *Advances in Space Research*, 11, 231-240.
- 576 Schwartz, S. J., Burgess, D., Wilkinson, W. P., Kessel, R. L., Dunlop, M., & Luehr,
577 H. (1992, April). Observations of short large-amplitude magnetic structures at
578 a quasi-parallel shock. *J. Geophys. Res.*, 97, 4209-4227.
- 579 Shan, L., Lu, Q., Wu, M., Gao, X., Huang, C., Zhang, T., & Wang, S. (2014, Jan-
580 uary). Transmission of large-amplitude ULF waves through a quasi-parallel
581 shock at Venus. *Journal of Geophysical Research (Space Physics)*, 119, 237-
582 245. doi: 10.1002/2013JA019396
- 583 Shan, L., Mazelle, C., Meziane, K., Romanelli, N., Ge, Y. S., Du, A., ... Zhang, T.
584 (2018, January). The Quasi-monochromatic ULF Wave Boundary in the Venu-
585 sian Foreshock: Venus Express Observations. *Journal of Geophysical Research*
586 *(Space Physics)*, 123(1), 374-384. doi: 10.1002/2017JA024054
- 587 Shuvalov, S. D., & Grigorenko, E. E. (2023). Observation of slams-like structures
588 close to martian aphelion by maven. *Journal of Geophysical Research: Space*
589 *Physics*, 128(5), e2022JA031018.
- 590 Slavin, J. A., Elphic, R. C., Russell, C. T., Scarf, F. L., Wolfe, J. H., Mihalov, J. D.,
591 ... Daniell, R. E. (1980, December). The solar wind interaction with Venus -
592 Pioneer Venus observations of bow shock location and structure. *J. Geophys.*
593 *Res.*, 85, 7625-7641.
- 594 Smith, E. J., Davis, L., Jr., Coleman, P. J., Jr., & Sonett, C. P. (1965a, April).
595 Magnetic Measurements near Venus. *J. Geophys. Res.*, 70, 1571-1586.
- 596 Stakhiv, M., Landi, E., Lepri, S. T., Oran, R., & Zurbuchen, T. H. (2015,
597 March). On the Origin of Mid-latitude Fast Wind: Challenging the Two-
598 state Solar Wind Paradigm. *Astrophysical Journal*, 801(2), 100. doi:
599 10.1088/0004-637X/801/2/100
- 600 Sønnerup, B., & Scheible, M. (1998, January). Analysis Methods for Multi-
601 Spacecraft Data. In G. Paschmann & P. W. Daly (Eds.), (Vol. 1, chap. 8).
602 ISSI Scientific Reports Series SR-001.
- 603 Takahashi, K., McPherron, R. L., & Hughes, W. J. (1984, August). Multispacecraft
604 observations of the harmonic structure of Pc 3-4 magnetic pulsations. *J. Geo-*
605 *phys. Res.*, 89(A8), 6758-6774. doi: 10.1029/JA089iA08p06758
- 606 Thomsen, M. F., Thomas, V. A., Winske, D., Gosling, J. T., Farris, M. H., & Rus-
607 sell, C. T. (1993, September). Observational test of hot flow anomaly forma-
608 tion by the interaction of a magnetic discontinuity with the bow shock. *J.*
609 *Geophys. Res.*, 98, 15319-+. doi: 10.1029/93JA00792
- 610 Tsubouchi, K., & Lembège, B. (2004, February). Full particle simulations of short
611 large-amplitude magnetic structures (SLAMS) in quasi-parallel shocks. *Journal*
612 *of Geophysical Research (Space Physics)*, 109(A18), 2114.
- 613 Tsurutani, B. T., Arballo, J. K., Smith, E. J., Southwood, D., & Balogh, A. (1993,
614 November). Large-amplitude magnetic pulses downstream of the Jovian bow
615 shock: Ulysses observations. *Planet. Space. Sci.*, 41, 851-856.
- 616 Tsurutani, B. T., Smith, E. J., Thorne, R. M., Gosling, J. T., & Matsumoto, H.
617 (1987, October). Steepened magnetosonic waves at Comet Giacobini-Zinner. *J.*
618 *Geophys. Res.*, 92, 11074-11082.

- 619 Wilson, L. B., Koval, A., Sibeck, D. G., Szabo, A., Cattell, C. A., Kasper, J. C., ...
620 Wilber, M. (2013, March). Shocklets, SLAMS, and field-aligned ion beams
621 in the terrestrial foreshock. *Journal of Geophysical Research (Space Physics)*,
622 *118*(3), 957-966. doi: 10.1029/2012JA018186
- 623 Wilson, L. B., III, Cattell, C. A., Kellogg, P. J., Goetz, K., Kersten, K., Kasper,
624 J. C., ... Meziane, K. (2009, October). Low-frequency whistler waves and
625 shocklets observed at quasi-perpendicular interplanetary shocks. *J. Geophys.*
626 *Res.*, *114*(A13), 10106.
- 627 Zhang, T. L., Baumjohann, W., Delva, M., Auster, H.-U., Balogh, A., Russell, C. T.,
628 ... Lebreton, J.-P. (2006, November). Magnetic field investigation of the
629 Venus plasma environment: Expected new results from Venus Express. *Planet.*
630 *Space. Sci.*, *54*, 1336-1343.